Heat transfer in a tapered passage

Yasuaki Shiina*

Heat transfer to laminar flow in tapered passages is studied for two types of thermal boundary conditions: prescribed heat flux on both walls, and on one wall with the other wall adiabatic. In the analysis, the flow is assumed to be purely radial. Temperature distributions and Nusselt number are obtained for the heat flux $q \propto r^{\delta}$. The Nusselt number depends on Reynolds number and taper angle. The fully developed Nusselt number decreases with increase in δ for converging flow and increases for diverging flow. Constant heat flux boundary conditions, $\delta=0$, for converging flow yield a reduction in Nusselt number when compared with the case of parallel channel flow.

Keywords: *laminar heat transfer, accelerated flow, declerated flow, tapered passages*

Introduction

Laminar heat transfer in channels has been studied by many investigators since Graetz obtained a solution for flow in a circular pipe with constant wall temperature. A lot of effort has been devoted to the study of heat transfer in passages of constant cross-section, such as a circular pipe[1], a parallel channel[2], and annulus[3] and other configurations[4,5].

Laminar heat transfer in passages of longitudinally varying cross-section may be different from that in the case of constant cross-section. Walker and Rishehri[6] suggested that the boundary condition of constant heat flux brought about a lower Nusselt number for sink flow than for parallel channel flow. For the case of turbulent heat transfer with constant wall heat flux in a convergent channel preceded by a parallel channel, it was reported that the Nusselt number became lower in the convergent channel than in the parallel channel[7,8]. This decrease in Nusselt number may be caused not only by laminarization due to flow acceleration but also by the characteristics of the thermal boundary condition of the flow in tapered passages. Therefore, basic study of laminar heat transfer in a tapered passage may aid our understanding of turbulent heat transfer in accelerated flow, or heat transfer in passages of varying cross-section.

Few papers have dealt with laminar heat transfer in tapered passages. Millsaps and Pohlhausen[9] solved the momentum and energy equations in tapered passages, but their study was not concerned with the heat transfer from the walls. The first analysis known to the author is that of Sparrow and Starr[10]. They obtained fully developed Nusselt numbers with wall heat flux $q \propto 1/r$ and constant wall temperature using an approximate solution of the flow profiles. Their results show a higher Nusselt number for converging flow and a lower Nusselt number for diverging flow than for parallel channel flow. Yang and Price[11] obtained numerical solutions of velocity distributions and an average Nusselt number for uniform wall temperature and uniform inlet velocity. Dey and Nath[12] presented the temperature profiles in a thermal boundary layer of a convergent channel using a boundary-layer-type velocity profile, and indicated that one could expect higher heat transfer rates in convergent channel flow with constant wall temperature.

In the present study, heat transfer to laminar flow in tapered passages is solved with prescribed wall heat flux on both walls and on one wall with the other wall adiabatic. The method was then extended to determine the fully developed Nusselt number for the case of constant wall temperature.

* Heat Transfer Laboratory, Division of High Temperature Engineering, Japan Atomic Energy Research Institute, Tokai-Mura, Naka-Gun, Ibaraki-Ken 319-11, Japan

0142–727X/87/010064–08$3.00

Velocity profiles

The polar coordinate (r, θ) geometry of the system is illustrated in Fig 1. Assuming that the flow is purely radial in a tapered passage with angle 2α, the velocity component (v_r, v_θ) will be $v_r = u(r, \theta)$ and $v_\theta = 0$. The conservation laws for mass and momentum are written as follows:

$$\frac{1}{r}\frac{\partial(ru)}{\partial r}=0$$

$$u\frac{\partial u}{\partial r}=-\frac{1}{\rho}\frac{\partial p}{\partial r}+\nu\left(\frac{\partial^2 u}{\partial r^2}+\frac{1}{r}\frac{\partial u}{\partial r}+\frac{1}{r^2}\frac{\partial^2 u}{\partial \theta^2}-\frac{u}{r^2}\right) \tag{1}$$

$$0=-\frac{1}{\rho r}\frac{\partial p}{\partial \theta}+\nu\frac{1}{r^2}\frac{\partial u}{\partial \theta}$$

From the mass conservation equation, one can set

$$u=\frac{\nu f(\theta)}{r} \tag{2}$$

The sign of u is taken as positive for outflow and negative for inflow. We introduce the mean velocity u_m and dimensionless velocity $g(\theta)$ normalized by u_m:

$$u_m=\frac{1}{2r\alpha}\int_{-\alpha}^{+\alpha} ur\,d\theta \tag{3a}$$

$$g(\theta)=u/u_m \tag{3b}$$

We also introduce the variable $\xi=\theta/\alpha$ and the Reynolds number based on the local mean velocity and twice the local channel width

$$Re=\frac{u_m D}{\nu}=\frac{u_m 4r\alpha}{\nu} \tag{3c}$$

Elimination of the pressure term from Eq (1) gives

$$\frac{d^2 g}{d\xi^2}+4\alpha^2 g+\frac{Re\,\alpha}{4}g^2+\frac{8\alpha^3}{Re}A=0 \tag{4}$$

$(g=0 \text{ at } \xi=\pm 1)$

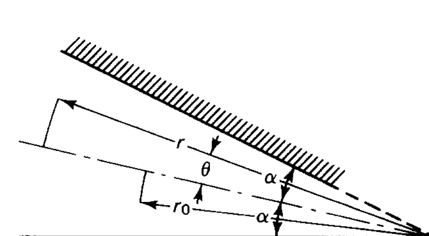

Figure 1 Schematic diagram of physical system

$$\int_{-1}^{+1} g\,d\xi = 2 \tag{5}$$

where A is a constant dependent on Re and α. Eq (4) was solved by Rosenhead[13] and Millsaps and Pohlhausen[9] using an elliptic function. In the present study, it was solved using a finite difference method. For the limiting case of α and Re, Eq (4) can be linearized and the problem becomes quite simple to solve.

(i) For the case of $\alpha=0$ (plane-Poiseuille flow)

$$g=3(1-\xi^2)/2 \tag{6}$$

(ii) For the case of $Re\to 0$ (Stokes flow)

$$g=\frac{2\alpha(\cos 2\alpha-\sin 2\alpha\xi)}{2\alpha\cos 2\alpha-\sin 2\alpha} \tag{7}$$

The velocity distributions are shown in Fig 2. The velocity is normalized by the centreline velocity u_c. Broken and dotted lines show the Poiseuille and Stokes flow profiles, respectively. The profiles B to D were compared with the results of Millsaps and Pohlhausen[9], which agree with the present results. For accelerated flow (inflow), the boundary layer becomes thinner and the velocity profiles flatter than the Poiseuille parabola with increase in $|Re|\alpha$. The limit as $|Re|\alpha\to\infty$ yields $g\to 1$. For decelerated flow (outflow) with small α and $Re\,\alpha$, the flow is unidirectional and the profiles are more sharply curved in the middle of the channel than the Poiseuille parabola. When $Re\,\alpha$ exceeds a critical value, however, there are certain regions in the cross-section where $g<0$ (curve A) and the solutions presented are not valid.

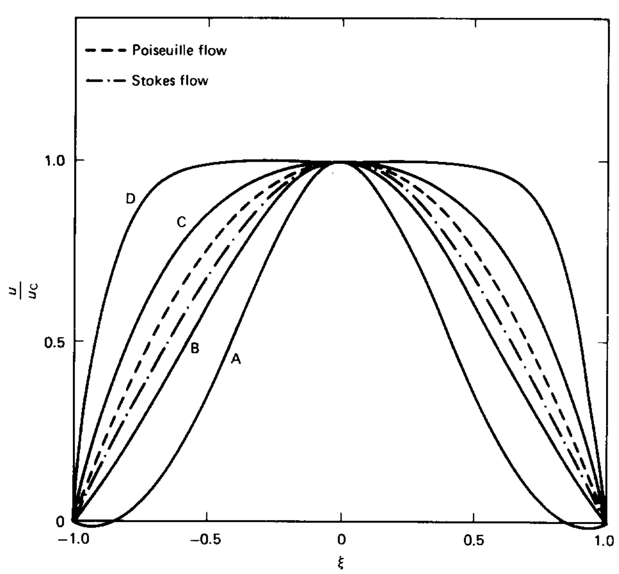

Figure 2 Velocity profiles in a tapered passage. Profiles B to D are comparable with the results of Millsaps and Pohlhausen[9]. A: $\alpha=0.01$, $Re=2000$. B to D: $\alpha=0.0873$ (5°), B: $Re=136$ ($R_c=u_c r/\nu=684$), C: $Re=-176$ ($R_c=-684$), D: $Re=-1527$ ($R_c=-5000$)

Heat transfer

If the viscous dissipation and axial heat conduction in the flow direction are neglected one finds the simple form of the energy equation to be

$$u\frac{\partial T}{\partial r}=\frac{\kappa}{r^2}\frac{\partial^2 T}{\partial \theta^2} \tag{8}$$

The wall is heated from $r=r_0$ to $r=0$ for inflow and from $r=r_0$ to $r=\infty$ for outflow. The following dimensionless variables are introduced:

$$\bar{r}=r/r_0=\exp(-\alpha t)\quad \text{(inflow)}$$
$$=\exp(\alpha t)\quad \text{(outflow)} \tag{9a}$$

$$\bar{T}=\frac{(T-T_i)\lambda}{q_0 r_0 \alpha} \tag{9b}$$

where $t=0$ for $\bar{r}=1$ and $t\to\infty$ for $\bar{r}\to 0$ for inflow or $r\to\infty$ for outflow. Substituting Eq (9) into Eq (8), we obtain

$$|Re|Pr\,g(\xi)\frac{\partial \bar{T}}{\partial t}=4\frac{\partial^2 \bar{T}}{\partial \xi^2} \tag{10}$$

Since Eq (10) is linear, the temperature profile for the prescribed wall heat flux can be obtained from the fundamental solution. Therefore, the initial step is to solve Eq (10) with the boundary condition of $\partial\bar{T}/\partial\xi=\pm 1$ on the wall. Since the wall heat flux is obtained using the temperature gradient in the fluid at the wall, $q=-\lambda r^{-1}(\partial T/\partial\theta)_{\theta=\pm\alpha}$, then $\partial\bar{T}/\partial\xi=\pm 1$ corresponds to $q\propto 1/r$.

Heat flux $q\propto 1/r$ on both walls

Eq (10) is identical to the energy equation of laminar heat transfer in a parallel channel except for the difference in the velocity profile $g(\xi)$. In this case, the heat flux can be expressed as $q=q_0/\bar{r}$. The boundary conditions are

$$t=0\ (\bar{r}=1)\quad \bar{T}(t,\xi)=0$$
$$t>0\quad \xi=\pm 1\quad \frac{\partial \bar{T}}{\partial \xi}=\pm 1 \tag{11}$$

Notation

C_n	Constant obtained from Eq (19)
D	Local hydraulic diameter $\equiv 4r\alpha$
g	Dimensionless velocity $\equiv u/u_m$
h_c	Heat transfer coefficient
Nu	Nusselt number $\equiv h_c D/\lambda$
Nu_0	Fully developed Nusselt number
P	Static pressure
Pr	Prandtl number
q	Heat flux
q_0	Dimensional constant of heat flux
r	Radial coordinate
$\bar{r}$	Dimensionless radial coordinate
r_0	r value at start of heating
Re	Reynolds number $\equiv u_m D/\nu$
t	Dimensionless variable defined by Eq (9a)
$T, \bar{T}$	Dimensional and dimensionless temperature, respectively
T_i	Inlet fluid temperature
$T_m, \bar{T}_m$	Dimensional and dimensionless mixed average temperature, respectively
$T_w, \bar{T}_w$	Dimensional and dimensionless wall temperature, respectively
u	Radial velocity
u_c	Centreline velocity
u_m	Mean velocity
Y_n	Eigenfunction
α	Half angle of tapered passage
β_n	Eigenvalue
δ	Arbitrary real number
λ	Thermal conductivity
θ	Angular coordinate
κ	Thermal diffusivity
ν	Kinematic viscosity
ξ	Dimensionless angular coordinate $\equiv\theta/\alpha$
ρ	Density
ϕ_1	Constant

It is well known that the heat transfer coefficient will approach a limiting value for a sufficiently large value of t, and the temperature profiles will tend to some similar shape. The similar temperature profile at sufficiently large t will be denoted by $\bar{T}_2$. The solution for $\bar{T}$ is written as

$$\bar{T}=\bar{T}_1+\bar{T}_2 \tag{12}$$

where $\bar{T}_1$ is simply the difference in the temperature profile after $\bar{T}_2$ is subtracted from $\bar{T}$, and it will approach zero at a sufficiently large value of t. Since Eq (10) is linear, it can be applied separately to $\bar{T}_1$ and $\bar{T}_2$. We thus obtain

$$|Re|Pr\, g(\xi)\frac{\partial \bar{T}_1}{\partial t}=4\frac{\partial^2 \bar{T}_1}{\partial \xi^2}$$

$$|Re|Pr\, g(\xi)\frac{\partial \bar{T}_2}{\partial t}=4\frac{\partial^2 \bar{T}_2}{\partial \xi^2} \tag{13}$$

For sufficiently large values of t, the temperature rise $\partial\bar{T}/\partial t$ is constant. Then

$$\bar{T}_2=Ct+\phi_1(\xi) \tag{14}$$

By integrating Eq (10) across the cross-section from $\xi=0$ to 1, we obtain

$$|Re|Pr\int_0^{+1} g(\xi)\frac{\partial \bar{T}}{\partial t}\,d\xi=4 \tag{15}$$

After substituting Eq (14) into Eqs (10) and (15), we find

$$C=\frac{4}{|Re|Pr\,\alpha} \tag{16a}$$

$$g(\xi)=\frac{d^2\phi_1}{d\xi^2}\quad\left(\xi=\pm 1, \frac{d\phi_1}{d\xi}=\pm 1\right) \tag{16b}$$

In order to obtain the solution $\bar{T}_1$, let $\bar{T}_1=R(t)\theta(\xi)$, and the separation of variables gives

$$\frac{dR}{dt}+\frac{4\beta}{|Re|Pr}R=0 \tag{17a}$$

$$\frac{d^2\theta}{d\xi^2}+\beta g(\xi)\theta=0 \tag{17b}$$

The application of the boundary conditions for $\bar{T}$ and $\bar{T}_2$, Eqs (11) and (16b), leads to the requirement that

$$\partial\bar{T}_1/\partial\xi=0 \quad \text{at } \xi=\pm 1 \tag{18}$$

By the integration of Eqs (17a) and (17b), we find

$$\bar{T}_1=\sum_1^{\infty} C_n Y_n(\xi)\exp\left(\frac{4\beta_n}{|Re|Pr}t\right)$$

where β_n and Y_n are the eigenvalues and eigenfunctions obtained from Eq (17b). The constant C_n is calculated from the equation

$$C_n=-\frac{\int_{-1}^{1}\phi_1 g Y_n\,d\xi}{\int_{-1}^{1} g T_n^2\,d\xi} \tag{19}$$

There $\bar{T}$ is written as

$$\bar{T}(t,\xi)=\sum_1^{\infty} C_n Y_n(\xi)\exp\left\{-\frac{4\beta_n t}{|Re|Pr}\right\}+\frac{4}{|Re|Pr}t+\phi_1(\xi) \tag{20a}$$

or

$$\bar{T}(\bar{r},\xi)=\sum_1^{\infty} C_n Y_n(\xi)\bar{r}^{-\frac{4\beta_n}{Re\,Pr\,\alpha}}+\frac{4}{Re\,Pr\,\alpha}\ln\bar{r}+\phi_1(\xi) \tag{20b}$$

After multiplying Eq (20b) by $g(\xi)$ and letting $\bar{r}=1$, an integration from $\xi=-1$ to 1 yields

$$\int_{-1}^{1} g\phi_1\,d\xi=0 \tag{21}$$

The local heat transfer coefficient h_c and Nusselt number are defined as

$$h_c\equiv\frac{q}{T_w-T_m},\qquad \mathrm{Nu}\equiv\frac{h_c D}{\lambda} \tag{22}$$

where T_w is the wall temperature ($\xi=\pm 1$) and T_m is the bulk temperature of the fluid expressed as

$$T_m=\frac{\int_{-\alpha}^{\alpha} Tu\,r\,d\theta}{\int_{-\alpha}^{\alpha} u\,r\,d\theta}=\frac{1}{2}\int_{-1}^{1} Tg\,s\xi \tag{23}$$

The use of the dimensionless form of the temperature defined in Eq (9b), and $D=4r\alpha$, with $q=q_0/\bar{r}$, yields

$$Nu=\frac{4}{\bar{T}_w-\bar{T}_m},\quad \bar{T}_m=\frac{4}{Re\,Pr\,\alpha}\ln\bar{r} \tag{24}$$

Upon substitution of Eqs (20a) and (20b) into Eq (24), one finds

$$Nu=\frac{4}{\sum_1^{\infty} C_n Y_n(1)\bar{r}^{-4\beta_n/(Re\,Pr\,\alpha)}+\phi_1(1)} \tag{25}$$

For $\bar{r}\to 0$ (inflow) or $\bar{r}\to\infty$ (outflow), the Nusselt number converges to a value independent of $\bar{r}$. It is called the 'fully developed' Nusselt number in the present study and is represented by Nu_0. It is obtained using

$$Nu_0=4/\phi_1(1) \tag{26}$$

For particular cases, Nu_0 can be easily obtained as follows. (i) $\alpha=0$ (parallel channel); combination of Eqs (6), (16b) and (21) yields

$$\phi_1=-\frac{\xi^4}{8}+\frac{3\xi^2}{4}-\frac{39}{280} \tag{27}$$

$$Nu_0=8.235$$

(ii) $Re\,\alpha\to-\infty$: combination of Eqs (16b) and (21) with $g=1$ gives

$$\phi_1=\frac{\xi^2}{2}-\frac{1}{6}$$

$$Nu_0=12 \tag{28}$$

(iii) $Re\to 0$ (Stokes flow): combination of Eqs (7), (16b) and (21) yields

$$\phi_1=B\left(\frac{\xi^2}{2}+\frac{\cos 2\alpha\xi}{4\alpha^2\cos 2\alpha}\right)+\frac{5B^2}{6}+B\left(\frac{3}{8\alpha^2}-\frac{3}{2}\right)+\frac{1}{2}$$

$$Nu_0=4/\{5B^2/6+B(5\alpha^2/8-1)+1/2\} \tag{29}$$

$$B=\frac{1}{(1-\tan 2\alpha)/2\alpha}$$

Fig 3 shows the relation between the Nusselt number and ln $(\bar{r}/(Re\,Pr\,\alpha)$ with $Re\,\alpha$ as a parameter for small α. The solid and broken lines in the figure are for the cases for inflow and outflow, respectively. Hereafter, the Prandtl number is fixed as 0.72, which is the value of air. With an increase in $|Re|\alpha$, the Nusselt number increases for inflow and decreases for outflow. The Nusselt number decreases with increases in $\ln\bar{r}/(Re\,Pr\,\alpha)$ and converges to a fully developed value. In the present study, we call the region where the Nusselt number is dependent on $\bar{r}$ as the 'thermal entry region'.

Values of the eigenvalues and eigenfunctions are presented in Table 1. The eigenvalues and eigenfunctions for the case of $Re\,\alpha\to-\infty$ can be obtained analytically. Upon integration of Eqs (17b) and (19) with $g=1$, we find

$$\beta_n=n^2\pi^2$$

$$Y_n=\cos n\pi\xi\quad (n=1,2,\ldots) \tag{30}$$

$$C_n=(-1)^{n+1}\frac{2}{(n\pi)^2}$$

Heat flux $q \propto r^{\delta}$ on both walls

Since the heat flux is expressed as $q = q_0 r^{\delta}$, the boundary conditions can be written as

$$\frac{\partial \bar{T}}{\partial \xi} = \pm e^{-\alpha(\delta+1)t} = \pm \bar{r}^{\delta+1}$$
at $= \pm 1$ (outflow)
$$\frac{\partial \bar{T}}{\partial \xi} = \pm e^{+\alpha(\delta+1)t} = \pm \bar{r}^{\delta+1} \tag{31}$$
at $\xi = \pm 1$ (inflow)

After rewriting $\bar{T}(t, \xi)$ in Eq (20) as $\bar{T}_0(t, \xi)$ the dimensionless temperature profiles with wall heat flux $q \propto r^{\delta}$ can be obtained from the formula

$$\bar{T}(t, \xi) = \bar{T}_0(t, \xi) - \alpha(\delta+1) \times \int_0^t e^{-\alpha(\delta+1)\tau}\, \bar{T}_0(t-\tau, \xi)\, d\tau \text{ (inflow)}$$
$$\bar{T}(t, \xi) = \bar{T}_0(t, \xi) + \alpha(\delta+1) \times \int_0^t e^{\alpha(\delta+1)\tau}\, \bar{T}_0(t-\tau, \xi)\, d\tau \text{ (outflow)} \tag{32}$$

After integration of Eq (32), the transformation of t into $\bar{r}$ yields

$$\bar{T}(\bar{r}, \xi) = \sum_1^{\infty} C_n Y_n(\xi) \bar{r}^{-4\beta_n/(Re\,Pr\,\alpha)} \times \left\{\frac{4\beta_n}{(1+\delta)Re\,Pr\,\alpha + 4\beta_n}\right\} + \sum_1^{\infty} C_n Y_n(\xi) \bar{r}^{\delta+1} \times \left\{\frac{(1+\delta)Re\,Pr\,\alpha}{(1+\delta)Re\,Pr\,\alpha + 4\beta_n}\right\} + \frac{1}{(1+\delta)Re\,Pr\,\alpha}(\bar{r}^{\delta+1} - 1) + \phi_1(\xi)\bar{r}^{\delta+1} \tag{33}$$

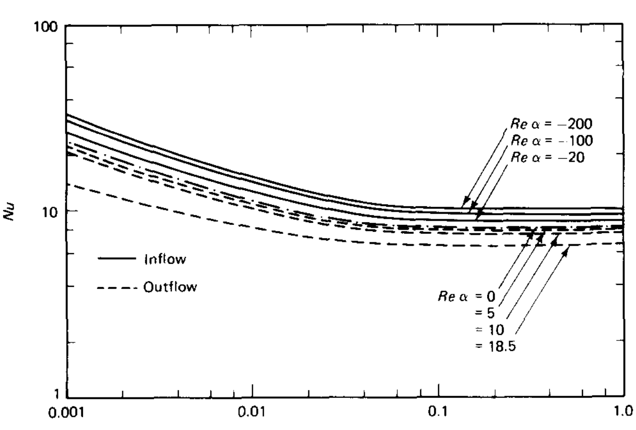

Figure 3 Relation between Nu and $\ln \bar{r}/Re\,Pr\,\alpha$ with heat flux $q \propto 1/r$ on both walls for small α

When $\delta = -1$, the third term of the right hand side of Eq (26) reduces to $4 \ln \bar{r}/(Re\,Pr\,\alpha)$. The Nusselt number is obtained as

$$Nu = 4 \Bigg/ \left[\sum_1^{\infty} C_n Y_n(1) \bar{r}^{-4\beta_n/(Re\,Pr\,\alpha) - 1 - \delta} + \left\{\frac{4\beta_n}{(1+\delta)Re\,Pr\,\alpha + 4\beta_n}\right\} + \sum_1^{\infty} C_n Y_n(1) \times \left\{\frac{(1+\delta)Re\,Pr\,\alpha}{(1+\delta)Re\,Pr\,\alpha + 4\beta_n}\right\} + \phi_1(1)\right] \tag{34}$$

For the case of $\delta > -1$ at $\bar{r} \to 0$ (inflow) or $\delta < -1$ at $\bar{r} \to \infty$ (outflow), Eq (33) reduces to

$$\bar{T}(\bar{r}, \xi) = -\frac{4}{(1+\delta)Re\,Pr\,\alpha} \tag{35}$$

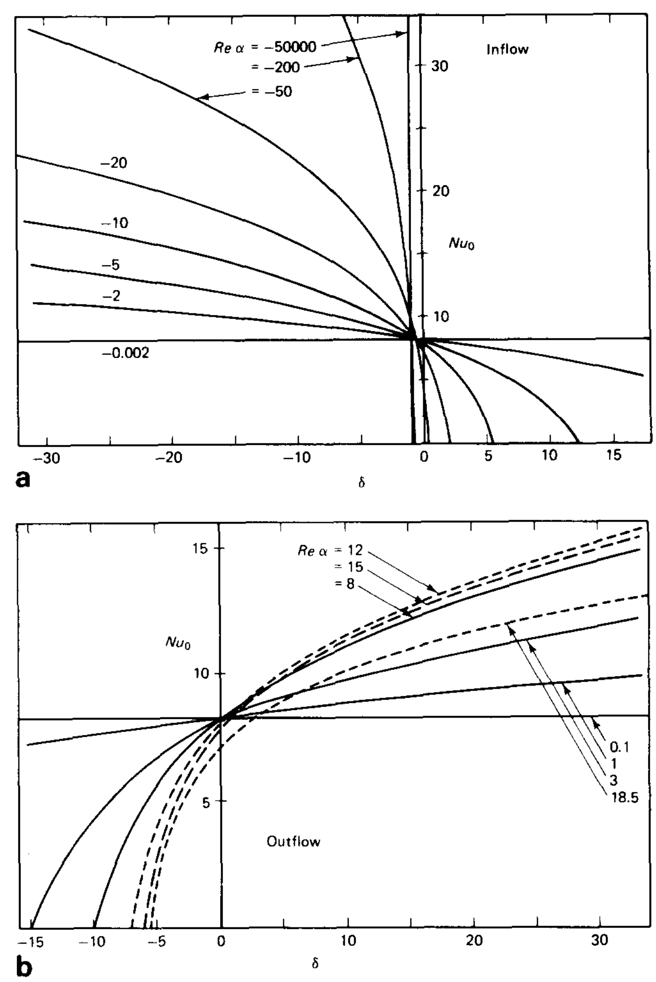

Figure 4 Effect of δ on Nu_0 for small α with $Re\,\alpha$ as a parameter: (a) inflow; (b) outflow

Table 1 Eigenvalues and related constants with both walls heated

	$\alpha=0$		$Re\,\alpha=-2000(\alpha=1.0)$		$Re\,\alpha=18.5$	
n	β_n	$C_nY_n(1)$	β_n	$C_nY_n(1)$	β_n	$C_nY_n(1)$
1	12.2527369	−0.222194	10.2152081	−0.197778	15.4346171	−0.218361
2	45.9512137	−0.072519	40.7878004	−0.050974	55.5509695	−0.083379
3	100.9465197	−0.037364	91.5477671	−0.023636	120.2866612	−0.046592
4	177.1635513	−0.023283	162.3116433	−0.013942	209.5349664	−0.030638
5	274.5076115	−0.016116	252.9209723	−0.009363	323.1461701	−0.022066
6	392.8602413	−0.011927	363.2376661	−0.006814	460.9286537	−0.016844
7	532.0782972	−0.009245	493.1278875	−0.005237	622.6485461	−0.013381
8	691.9937038	−0.007413	642.4500057	−0.004186	808.0301953	−0.010962
9	872.4134248	−0.006108	811.0482207	−0.003447	1016.7562494	−0.009182
10	1073.1195299	−0.005127	998.7497133	−0.002906	1248.4677830	−0.007830

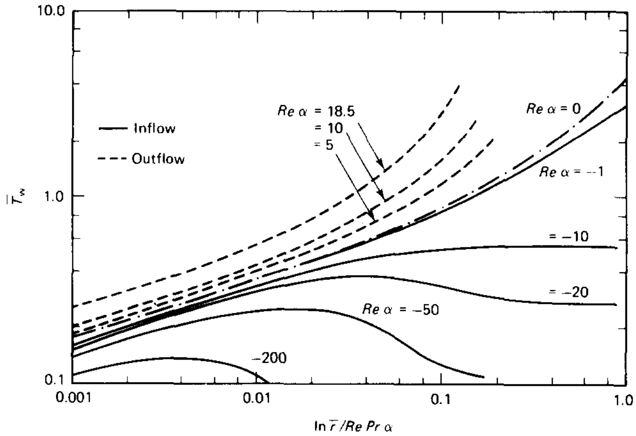

Figure 5 Plot of dimensionless wall temperature against $\ln \bar r/Re\,Pr\,\alpha$ for case of constant heat flux ($\delta = 0$), with both walls heated, for small α

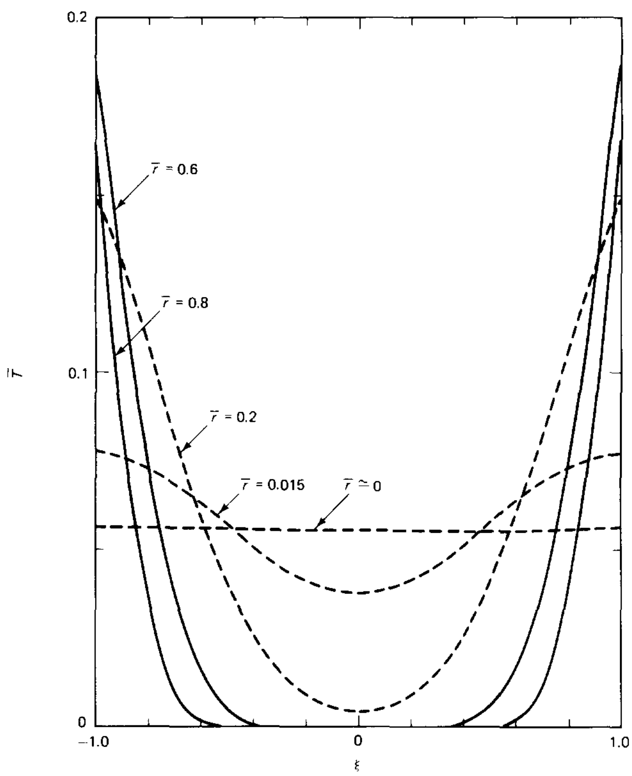

Figure 6 Temperature profiles in fluid with constant heat flux (both walls heated) for case of $\alpha = 0.1$ and $Re = -1000$. Broken lines are the profiles when wall temperature is decreasing towards $\bar r \to 0$

ie the temperature profile becomes uniform in this region. In other regions of δ, the temperature profile is dependent on $\bar r$.

When $\delta \leqslant -1$ for inflow and $\delta \geqslant -1$ for outflow, $\bar r^{-4\beta_n/(Re\,Pr\,\alpha)-1-\delta}$ always converges to 0 as $\bar r \to 0$ for inflow and $\bar r \to \infty$ for outflow. Then the fully developed Nusselt number Nu_0 is obtained as

$$Nu_0 = 4\Big/\left\{\sum_1^{\infty} C_n Y_n(1)\frac{(1+\delta)Re\,Pr\,\alpha}{(1+\delta)Re\,Pr\,\alpha + 4\beta_n} + \phi_1(1)\right\} \tag{36}$$

Plots of Nu_0 against δ are shown in Figs 4(a) and 4(b) for inflow and outflow, respectively, for small α with $Re\,\alpha$ as a parameter. The Nusselt number Nu_0 is a monotonically decreasing function for inflow and a monotonically increasing function for outflow with respect to δ, as shown in the figures. For inflow, Nu_0 increases with increase in $|Re|\alpha$ for $\delta \leqslant -1$ and decreases for $\delta \gtrsim -0.3$. When $\delta = -1$, Nu_0 increases from 8.235 to 12 as $|Re|\alpha$ increases from 0 to ∞. For $\delta > -1$, there are values of $Re\,\alpha$ which yield $-4\beta_1/(Re\,Pr\,\alpha) - 1 - \delta < 0$ where β_1 is the smallest eigenvalue. This yields $Nu_0 = 0$.

On the contrary for outflow, Nu_0 decreases with $Re\,\alpha$ for $\delta \leqslant -1$ and increases with $Re\,\alpha$ for $\delta \gtrless 0$ for small values of $Re\,\alpha$. However, it decreases as $Re\,\alpha$ approaches the critical value above which flow is no longer unidirectional.

As described above, the Nusselt number in Eq (34) always converges to a value including zero at $\bar r \to 0$ (inflow) or $\bar r \to \infty$ (outflow). This means that there is always a fully developed Nusselt number for the case of heat flux $q \propto r^{\delta}$.

The relation between $\bar T_w$ and $\ln \bar r/(Re\,Pr\,\alpha)$ with constant wall heat flux ($\delta = 0$) is shown in Fig 5 for small α. The solid lines and broken lines represent the results for inflow and outflow, respectively. When $|Re|\alpha \ll 1$, the dimensionless wall temperature $\bar T_w$ increases with $\ln \bar r/(Re\,Pr\,\alpha)$. An increase in $|Re|\alpha$ yields a lower wall temperature for inflow and a higher wall temperature for outflow. When $|Re|\alpha$ exceeds a certain value for inflow, the wall temperature has a negative gradient towards the flow direction.

The temperature profiles in the fluid are shown in Fig 6 for the case of $Re\,\alpha = -100$ for inflow with constant heat flux. The same trend for the wall temperature as seen in Fig 5 for large values of $|Re|\alpha$ is shown in Fig 6. It is noteworthy that the temperature gradient is higher in the fluid near the walls than at the wall for the region of $\bar r \lessgtr 0.2$. This is due to the decrease in wall temperature in the flow direction. Dey and Nath[12] have reported that a rapid decrease in wall temperature for boundary-layer-type sink flow caused the fluid near the wall to be hotter than the wall itself. For this case, however, it does not occur because the decrease in the wall temperature is not large enough.

The relation between Nu and $\ln \bar r/Re\,Pr\,\alpha$ for small α with constant wall heat flux is shown in Figs 7(a) and 7(b) for inflow and outflow, respectively. In both figures, the solid line represents the case of $\alpha = 0$, which corresponds to the case of a parallel channel. It is worthy to note that the Nusselt number in

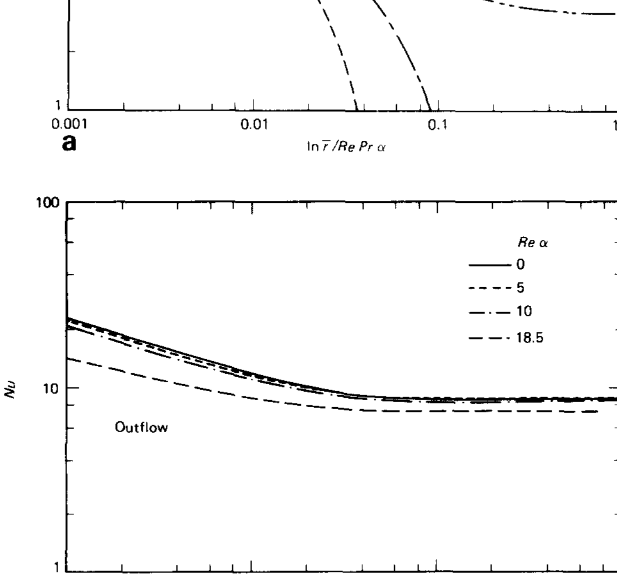

Figure 7 Relation between Nu and $\ln \bar r/Re\,Pr\,\alpha$ for small α with constant heat flux on both walls: (a) inflow; (b) outflow

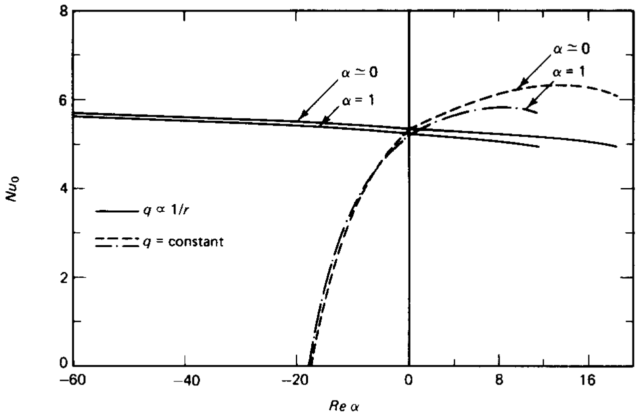

Figure 8 Relation between $Re\,\alpha$ and Nu_0 with both walls heated for cases of $\delta=-1$ and $\delta=0$

the entry region with constant q is higher for inflow and lower for outflow that in the entry region with $q \propto 1/r$, whereas the fully developed value Nu_0 with $q=$constant for inflow lies below Nu_0 with $q \propto 1/r$.

The plot of Nu_0 against $Re\,\alpha$ is shown in Fig 8 with δ and α as parameters. For the case of $\delta=-1$, Nu_0 increases with decrease in $Re\,\alpha$ and converges to 12 at $Re\,\alpha \to -\infty$. For the case of $\delta=0$, however, Nu_0 decreases with decrease in $Re\,\alpha$ for inflow and reduces to 0 for $Re\,\alpha \lessapprox -62.8$.

Heat flux on one wall with the other wall adiabatic

The calculation procedure for this case is the same as that described in the previous section. The temperature distribution can be expressed by Eqs (20)and (33), but in this case ϕ_1 is calculated by the following equation instead of Eq (16b)

$$g(\xi)=\frac{d^2\phi_1}{d\xi^2} \quad \xi=1: d\phi_1/d\xi=1$$
$$\xi=-1: d\phi_1/d\xi=0 \tag{37}$$

The Nusselt number can be obtained from Eq (25) for $\delta=-1$ and from Eq (34) for $\delta \neq -1$. For the case of $Re\,\alpha \to -\infty$, one can obtain, by using the same procedure as in the previous section,

$$\phi_2=\frac{\xi^2}{4}+\frac{\xi}{2}-\frac{1}{2}$$

$$Nu_0=6$$

The relation between $Re\,\alpha$ and Nu_0 is shown in Fig 9. Similar profiles to those in Fig 8 are seen in this figure. The value of $Re\,\alpha$ beyond which Nu_0 reduces to zero for inflow is smaller for this case than with the case of both walls heated. This is due to the difference of the smallest eigenvalue.

Eigenvalues and eigenfunctions for $Re\,\alpha \to -\infty$ are analytically obtained as follows:

$$\beta_n=\frac{(n\pi)^2}{4}$$

$$Y_n(\xi)=\cos(n\pi/2), \quad C_n=(-1)^{n+1}\frac{4}{(n\pi)^2},$$
$$(n=2m)$$
$$Y_n(\xi)=\sin(n\pi/2), \quad C_n=(-1)^{n+1}\frac{4}{(2n+1)^2\pi^2}, \tag{38}$$
$$(n=2m-1)$$

The case of constant wall temperature for inflow

Uniform temperature on both walls

Sparrow and Patankar[14] noted that the boundary condition of constant wall temperature for a circular pipe was identical to that of $q \propto \exp(\gamma x)$ for the fully developed region. As is pointed out by Walker and Rishehri[6], the boundary condition $q \propto e^{\gamma x}$ for parallel flow corresponds to the boundary condition of $q \propto r^{\gamma/4\alpha-1}$ for flow in a tapered passage if the difference in the velocity profiles is neglected. The heat transfer in tapered passages for inflow with constant wall temperature can be obtained using the results of the previous sections. We assume that the heat flux q can be described as $q=q_0 h(\bar{r})$ where $h(\bar{r})$ is an arbitrary function of $\bar{r}$. Instead of Eq (9b), the following dimensionless variables are introduced:

$$\bar{r}=r/r_0$$
$$\bar{T}=\frac{T-T_i}{T_w-T_i} \tag{39}$$

Upon substituting this into Eq (8), we again obtain Eq (10). By integrating it across the cross-section from $\xi=-1$ to 1, we obtain (see Appendix A)

$$Re\,Pr\,\alpha\frac{d\bar{T}_m}{d\bar{r}}=\frac{Nu}{\bar{r}}(1-\bar{T}_m) \tag{40}$$

It is assumed that a fully developed value of Nusselt number, Nu_0, exists at $r \to 0$. Substitution of Nu_0 into Eq (40) and then integrating yields

$$\bar{T}_m=1-C\bar{r}^{-Nu_0/(Re\,Pr\,\alpha)}$$

$$q=\frac{Nu_0}{4r_0\alpha}(T_w-T_i)\frac{\lambda}{\bar{r}}(1-\bar{T}_m) \propto \bar{r}^{-(Nu_0/Re\,Pr\,\alpha)-1}=\bar{r}^{\delta}$$

where C is a constant. From the above equations, we find δ is equal to $-(Nu_0/Re\,Pr\,\alpha)-1>-1$. Accordingly, we obtain

$$-\frac{4\beta_n}{Re\,Pr\,\alpha}-1-\delta=-\frac{1}{Re\,Pr\,\alpha}(4\beta_n-Nu_0)$$

Here $4\beta_n-Nu_0$ must be larger than zero for all n. If not, Nu_0 becomes zero and it yields $\delta=-1$, which means that Nu_0 will not be zero as described in the previous chapter.

The value of Nu_0 is obtained by the substitution of δ into Eq (34):

$$Nu_0=4\Bigg/\left[-\sum_1^{\infty}C_nY_n(1)\frac{Nu_0}{(4\beta_n-Nu_0)}+\phi_1(1)\right] \tag{41}$$

where ϕ_1 is obtained from Eq (16b).

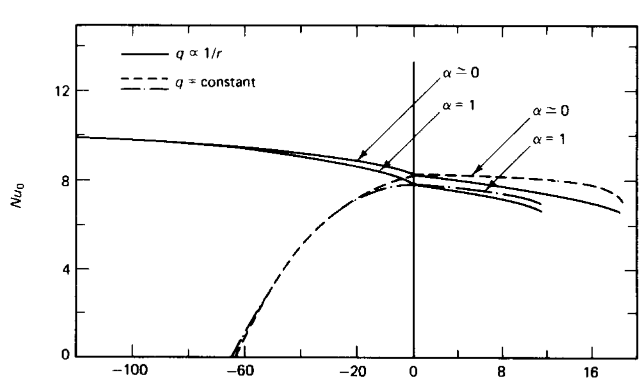

Figure 9 Relation between $Re\,\alpha$ and Nu_0 with one wall heated and the other wall adiabatic for cases of $\delta=-1$ and $\delta=0$

Here, we consider the case of $Re\,\alpha \to -\infty$. From Eq (30)

$$-\sum_{1}^{\infty} C_n Y_n(1) \frac{Nu_0}{(4\beta_n - Nu_0)} = -\frac{1}{3} + \frac{4}{Nu_0} - \frac{2\cot(\sqrt{Nu_0}/2)}{\sqrt{Nu_0}} \tag{42}$$

Solving the above equation, we obtain (see Appendix B)

$$Nu_0 = \pi^2 = 9.8696 \tag{43}$$

Uniform temperature on one wall with the other wall adiabatic

The following equations are obtained corresponding to the previous section

$$\bar{T}_m = 1 - C\bar{r}^{-Nu_0/(2Re\,Pr\,\alpha)}$$

$$q \propto \bar{r}^{-(Nu_0/2Re\,Pr\,\alpha)-1} \tag{44}$$

$$Nu_0 = 4\Bigg/\left[-\sum_{1}^{\infty} C_n Y_n(1) \frac{Nu_0}{(8\beta_n - Nu_0)} + \phi_1(1)\right]$$

where ϕ_1 is obtained from Eq (37). For the case of $Re\,\alpha \to -\infty$, we obtain

$$Nu_0 = \pi^2/2 = 4.9348 \tag{45}$$

Concluding remarks

Laminar heat transfer in a tapered passage is different from that in a parallel channel because of the dependence of the velocity distribution on the Reynolds number and taper angle. In the present analysis, temperature distributions and Nusselt number are obtained for the prescribed heat flux of $q \propto r^{\delta}$ on both walls and on one wall with the other wall adiabatic. The behaviour of the fully developed Nusselt number, Nu_0, depends on the value of δ. For inflow, Nu_0 increases for $\delta \leqslant -1$ and decreases for $\delta \gtrless -0.3$ with an increase in $Re\,\alpha$. On the contrary, for outflow, Nu_0 decreases for $\delta \leqslant -1$ with $Re\,\alpha$ and increases for $\delta \gtrless 0$ with $Re\,\alpha$; however, it decreases for $\delta \gtrless 0$ as $Re\,\alpha$ approaches the critical value above which flow is no longer unidirectional. Accordingly, for inflow with constant heat flux, Nu_0 converges to a lower value than that for the case of a parallel channel. If $Re\,\alpha$ satisfies $-4\beta_1/(Re\,Pr\,\alpha) - 1 - \delta < 0$, Nu_0 converges to zero.

The fully developed Nusselt number with constant wall temperature is easily calculated by using the eigenvalues and eigenfunctions which are obtained from the appropriate prescribed heat flux boundary condition.

References

1 Siegel, R., Sparrow, E. M. and Hallman, T. M. Steady laminar heat transfer in a circular tube with prescribed wall heat flux. *Appl. Sci. Res.*, 1958, **A7**, 386–392

2 Sellars, J. R., Tribus, M. and Klein, J. S. Heat transfer to laminar flow in a round tube or flat conduit—the Graetz problem extended. *Trans. ASME*, 1956, **78**, 441–448

3 Hatton, A. P. and Quarmby, A. Heat transfer in the thermal entry length with laminar flow in an annulus. *Int. J. Heat Mass Transfer*, 1962, **5**, 973–980

4 Dennis, S. C. R., Mercer, A. M. and Poots, G. Forced heat convection in laminar flow through rectangular ducts. *Q. Appl. Math.*, 1959, **17**, 285–297

5 Shah, R. K. Laminar flow friction and forced convection heat transfer in ducts of arbitrary geometry. *Int. J. Heat Mass Transfer*, 1975, **18**, 849–862

6 Walker, V. and Rishehri, S. A. Forced convection in parallel and tapered passages: the importance of the heat flux boundary condition. *Int. J. Heat Mass Transfer*, 1972, **15**, 781–788

7 Tanaka, H. and Shimizu, J. Laminarization in low Reynolds number turbulent duct flow. *Trans. ASME Ser. C*, 1977, **99**, 682–684

8 Tanaka, H., Kawamura, H., Tateno, A. and Hatamiya, S. Effect of laminarization and retransition on heat transfer for low Reynolds number flow through a converging to constant area duct. *Trans. ASME. Ser. C*, 1982, **102**, 363–371

9 Millsaps, K. and Pohlhausen, K. Thermal distribution in Jeffrey-Hamel flows between nonparallel plane walls. *J. Aeronaut. Sci.*, 1953, **20**, 187–196

10 Sparrow, E. M. and Star, J. B. Heat transfer to laminar flow in tapered passages. *J. Appl. Mech.*, 1965, **87**, 684–689

11 Yang, J. W. and Price, G. M. Laminar flow development and heat transfer in converging plane-walled channels. *Appl. Sci. Res.*, 1972, **25**, 361–371

12 Dey, J. and Nath, J. Boundary-layer convective heat transfer in a convergent channel. *Lett. in Heat Mass Transfer*, 1981, **8**, 371–377

13 Rosenhead, L. The steady two-dimensional radial flow of viscous fluid between two inclined plane walls. *Proc. R. Soc. (London) Ser. A*, 1940, **175**, 436–467

14 Sparrow, E. M. and Patankar, S. V. Relationships among boundary conditions and Nusselt numbers for thermally developed duct flows. *Trans. ASME. Ser. C*, 1977, **99**, 483–485

Appendix A: Derivation of Eq (40)

Integrating Eq (10) from $\xi = -1$ to 1 and converting t into $\bar{r}$, we obtain

$$Re\,Pr\,\alpha \int_{-1}^{1} g \frac{\partial \bar{T}}{\partial \bar{r}} d\xi = 4\frac{1}{\bar{r}}\left[\frac{\partial \bar{T}}{\partial \xi}\right]_{-1}^{1} \tag{A1}$$

Since the wall heat flux is written as

$$q = \pm\lambda \frac{1}{r}\left\{\frac{\partial T}{\partial \theta}\right\}_{\pm\alpha} = \pm\frac{\lambda(T_w - T_i)}{r_0\alpha\bar{r}}\left\{\frac{\partial \bar{T}}{\partial \xi}\right\}_{\xi=\pm 1}$$

we obtain

$$\frac{1}{\bar{r}}\left\{\frac{\partial \bar{T}}{\partial \xi}\right\}_{\pm 1} = \pm\frac{q r_0 \alpha}{\lambda(T_w - T_i)} \tag{A2}$$

Substitution of Eq (A2) into Eq (A1) yields

$$Re\,Pr\,\alpha \frac{d}{d\bar{r}} \int_{-1}^{1} g\bar{T}\, d\xi = \frac{2q r_0\alpha}{\lambda(T_w - T_i)} \tag{A3}$$

By using the dimensionless bulk temperature and the definition of the Nusselt number

$$\bar{T}_m = \frac{1}{2}\int g\bar{T}\, d\xi, \quad Nu = \frac{4r\alpha}{\lambda}\frac{q}{(T_w - T_m)}$$

we obtain from Eq (A3)

$$Re\,Pr\,\alpha \frac{d\bar{T}_m}{d\bar{r}} = \left(\frac{Nu}{\bar{r}}\right)\frac{T_w - T_m}{T_w - T_i} = \frac{Nu}{\bar{r}}(1 - \bar{T}_m) \tag{A4}$$

We now introduce the fully developed Nusselt number Nu_0. Integration of Eq (A4) yields

$$\bar{T}_m = 1 - C\bar{r}^{-Nu_0/(Re\,Pr\,\alpha)} \tag{A5}$$

Here, Nu_0 is expressed as

$$Nu_0 = \frac{4r\alpha q}{\lambda(T_w - T_m)}$$

Then

$$q = \frac{Nu_0\lambda(T_w - T_m)}{4r\alpha} = \frac{Nu_0\lambda(T_w - T_i)(1 - \bar{T}_m)}{4r_0\alpha\bar{r}} \tag{A6}$$

Substituting Eq (A5) into (Eq (A6), we obtain

$$q = CNu_0\lambda\frac{T_w - T_i}{4r_0\alpha}\bar{r}^{-(Nu_0/Re\,Pr\,\alpha)-1} \propto \bar{r}^{-(Nu_0/Re\,Pr\,\alpha)-1} \tag{A7}$$

Appendix B: Derivation of Eq (43)

The first term of the right hand side of Eq (41) is written as

$$-\sum_1^\infty C_n Y_n(1)\frac{Nu_0}{(Nu_0-4\beta_n)}$$
$$=\sum_1^\infty \frac{2}{(n\pi)^2}\frac{Nu_0}{(4n^2\pi^2-Nu_0)}$$
$$=\frac{2}{\pi^2}\sum_1^\infty\left[-\frac{1}{n^2}+\frac{1}{(n^2-Nu_0/4\pi^2)}\right] \tag{B1}$$

The right hand side of Eq (B1) becomes

$$\sum_1^\infty (1/n)^2=\pi^2/6$$

$$\sum_1^\infty \frac{1}{n^2-Nu_0/4\pi^2}=\frac{2\pi^2}{Nu_0}-\frac{\pi^2}{\sqrt{Nu_0}}\cot(\sqrt{Nu_0}/2)$$

Then we obtain

$$-\sum_1^\infty C_n Y_n(1)\frac{Nu_0}{4\beta_n-Nu_0}$$
$$=-\frac{1}{3}+\frac{4}{Nu_0}-\frac{2}{\sqrt{Nu_0}}\cot(\sqrt{Nu_0}/2) \tag{B2}$$

This corresponds to Eq (42). Substituting Eq (B2) into Eq (41), and considering that $\phi_1(1)=1/3$, we obtain

$$Nu_0=4\Big/\left[\frac{4}{Nu_0}-\frac{2}{\sqrt{Nu_0}}\cot(\sqrt{Nu_0}/2)\right] \tag{B3}$$

From Eq (B3), we obtain

$$\cot(\sqrt{Nu_0}/2)=0$$

Therefore

$$Nu_0=(2m+1)^2\pi^2 \quad (m=0,1,2,\ldots) \tag{B4}$$

where $4\beta_n-Nu_0$ must be larger than zero. Since the smallest value of $\beta_n=\pi^2$, m must be zero. Thence we obtain

$$Nu_0=\pi^2$$

Book review

Heat Conduction

S. Kakac and Y. Yener

This is a good book on heat conduction and is intended as a textbook for senior/first year graduate students in heat transfer and also as a reference for heat transfer engineers.

The book is similar in some respects to the text by P. J. Schneider. Extended surfaces and steady-state one-dimensional cases are covered, for example, in both books. Also the Heisler charts are given and the book displays other features that are helpful for engineering practitioners, such as thermal properties of some solids.

Good features of the book include an appropriate mathematical level and the good coverage of the major conventional topics. There is also an excellent chapter on further methods of solution besides the usual methods of separation of variables, integral transforms and Laplace transforms. These include Duhamel's method, the integral method, the variational method and methods for solving phase change problems. The writing style is good and the book is easy to read. Unfortunately the type design of the letters is not one of those commonly used in books.

The book shares some weaknesses with others on heat conduction and boundary value problems. One of these is the lack of explicit numerical evaluation of infinite series. Associated with this are occasional inaccurate statements regarding convergence. For example, on p. 202 it is stated that the series converge rapidly and satisfactory accuracy can be obtained with only a few terms; unfortunately one of the given equations cannot always be evaluated without using a great many terms. Another weakness is the omission of the Thomas algorithm for solving a tridiagonal set of algebraic equations in the finite difference chapter. It is only fair to note that no other advanced heat conduction book includes this important algorithm. Instead the authors mention solving the matrix equation

$$AT=C$$

by using the inverse A^{-1}, to obtain for the unknown temperature vector, T,

$$T=A^{-1}C$$

According to numerical analysis authors (see J. R. Rice, *Matrix Computations and Mathematical Software*, McGraw-Hill, 1981, p. 23) this an inefficient approach.

On the whole, the book is certainly a welcome addition to the heat transfer literature and can be very effectively used by both students and practicing engineers.

James V. Beck
Heat Transfer Group,
Department of Mechanical Engineering,
Michigan State University,
East Lansing, MI

Published price $37.50, by Hemisphere Publishing Corporation, 79 Madison Avenue, New York, NY 10016, USA, 397 pp.
This is an American review of a book previously reviewed in March 1986 by a UK reviewer.